VNU Journal of Science: Mathematics - Physics

Journal homepage: https://js.vnu.edu.vn/MaP

Original Article

Ni Stressor and h-BN Release Layer-assisted Mechanical Lift-off of GaN for Flexible Deep-UV Sensors on PET Substrates

Nguyen Hoang Hung[1,2], Nguyen Thien Trang[1,2], Kang Bok Ko[3], Huynh Vo Anh Hao[1,2], Tran Viet Cuong[1,2], Huynh Tran My Hoa[1,2,*]

[1]VKTECH Research Center, NTT Hi-Tech Institute, Nguyen Tat Thanh University, Vo Chi Cong, Tang Nhon Phu, Ho Chi Minh City, Vietnam

[2]Nguyen Tat Thanh University Center for Hi-Tech Development, Saigon Hi-Tech Park, Vo Chi Cong, Tang Nhon Phu, Ho Chi Minh City, Vietnam

[3]Semiconductor Physics Research Center, Jeonbuk National University, Jeonju 54896, Republic of Korea

Received 23rd March 2026
Revised 11th May 2026; Accepted 31st July 2026

Abstract: We present a two-step mechanical lift-off process for transferring GaN onto flexible polyethylene terephthalate (PET) substrates, utilizing a nickel (Ni) stressor layer and a hexagonal boron nitride (h-BN) release layer. An optimized Ni stressor layer thickness of 700 nm effectively reduces surface cracking when compared to thicknesses of 500 nm and 1000 nm. The surface quality of GaN is monitored throughout the experiments using an optical microscope (OM). Photoluminescence spectroscopy (PL) and UV-Vis measurements confirm that the optical bandgap of the transferred GaN on the PET substrate remains at 3.4 eV. A flexible GaN-based photoconductor that was fabricated exhibited a photoresponse at 254 nm, displaying a low dark current of 3.6×10^{-10} A and an on/off ratio of 2.97. This work highlights a straightforward and effective transfer method for the development of remote epitaxy GaN-based optoelectronic devices, particularly flexible ultraviolet photoconductors.

Keywords: h-BN; stressor layer; GaN; lift-off; remote epitaxy, deep-ultraviolet photoconductor.

[*] Corresponding author.
E-mail address: htmhoa@ntt.edu.vn

https//doi.org/10.25073/2588-1124/vnumap.5140

1. Introduction

Gallium Nitride (GaN) has been intensively studied over the past decades for multi-applications in optoelectronics and power electronic device [1-3]. Among these applications, its wide bandgap (~3.4 eV), excellent chemical stability, and radiation hardness make it particularly suitable for the active layer of optical sensor devices operating in ultraviolet spectral ranges [4-7]. Most recently, there is increasing interest in flexible deep ultraviolet (DUV) photodetectors for wearable and bendable devices [4, 8-11] due to their capable integration with other platforms to extend their application in healthcare and military systems. However, conventional GaN epitaxy was usually grown on rigid substrates such as sapphire, SiC or silicon that severely restricts flexibility and integration onto foreign platforms. Moreover, this epitaxy growth often requires high-temperatures, which are incompatible with transparent and flexible substrates due to thermal expansion mismatches and the mechanical deformation of those substrates.

To overcome this issue, chemical etching [12, 13], laser lift-off [14, 15], or dry etching with plasma [16, 17] and mechanical lift-off [18-20] approaches have been widely explored for the GaN transfer process. Although mechanical lift-off shows some advantages over chemical and laser processes, such as being a simple and scalable alternative, achieving reliable and damage-free mechanical separation of GaN remains challenging. It should be noted that mechanical lift-off strongly depends on controlled stress accumulation and crack propagation parallel to the main layer–substrate interface [18, 21]. Therefore, the success of mechanical lift-off relies heavily on selecting the right release layer and optimizing its thickness to control the crack density.

More recently, the two-dimensional material-assisted membrane transfer technique has emerged as a remote epitaxy mode. This approach maintains high-quality crystal growth while facilitating efficient membrane release and wafer reuse [22, 23]. Among two-dimensional materials, a two-dimensional hexagonal boron nitride (h-BN) interlayer promises to weaken interfacial bonding via van der Waals (vdWs) interactions and to mitigate thermal expansion mismatch and interfacial strain between the GaN layer and the sapphire substrate [24-29]. Inspired by this research, we herein demonstrate a stress-engineered mechanical lift-off strategy enabled by the combination of the h-BN release layer and a nickel (Ni) stressor layer. While h-BN suggests enhancing GaN crystalline quality and having a positive effect on the transfer process, the Ni overlayer introduces tunable tensile stress to promote controlled crack initiation and propagation to enhance transfer efficiency [30]. The combination between the h-BN release layer and the Ni stressor layer enables wafer-scale mechanical exfoliation of a high-quality GaN from the sapphire substrate and subsequently transfers it onto a flexible polyethylene terephthalate (PET) substrate to fabricate a flexible DUV photodetector. This process is detailed in a graphical abstract Fig. 1. The fabricated device exhibits current–voltage characteristics and reliable photoresponse under deep-UV illumination, demonstrating the viability of this approach for flexible GaN-based optoelectronic devices.

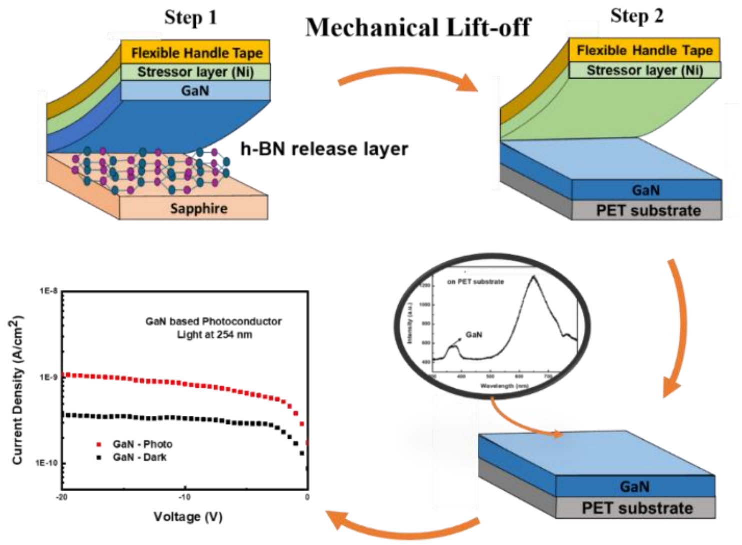

Figure 1. The graphical abstract in mechanical lift-off process for DUV photodetector.

2. Experimental Method

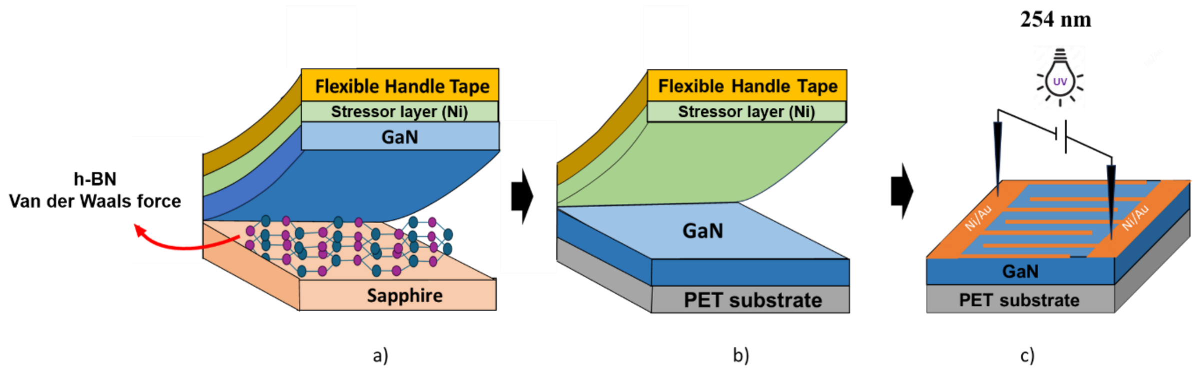

Figure 2. a) Schematic illustration of the Ni layer combination with 2D-hBN; b) Structure after lift-off process and c) DUV sensor with interdigitated top Ni/Au electrodes.

This study presents a straightforward lift-off GaN active layer for a deep ultraviolet sensor, utilizing a Ni stressor layer alongside a two-dimensional hexagonal boron nitride (h-BN) releasing layer. Fig. 2(a-c) depicts the newly established GaN lift-off technique for fabricating deep-ultraviolet sensors. An h-BN release layer was initially deposited, followed by a 2 µm-thick epitaxial GaN active layer on the sapphire substrate by metal organic chemical vapor deposition (MOCVD). The previous study provided comprehensive details regarding the MOCVD method [25]. We herein investigate the dependence of Ni stressor layer thickness on the GaN lift-off procedure. Ni films with thicknesses of 500 nm, 700 nm, and 1000 nm were deposited on the prepared GaN/h-BN/sapphire substrates utilizing a standard electron beam evaporation method. The initial phase of detaching the epitaxial GaN/Ni from the sapphire substrate, as depicted in Fig. 2(a), was entirely accomplished utilizing a flexible handling tape. This phase entailed a comprehensive examination of the influence of the Ni stressor layer thickness on lift-off GaN efficiency.The binding energy at the GaN/h-BN interface is inferior than that at the h-BN/sapphire interface, hence two-dimensional h-BN is pivotal as a shear plane. This resulted in the uniform and consistent exfoliation of epitaxial GaN/Ni (Fig. 2(b)). During the second stage of exfoliation, the Ni stressor layers were removed by consequently using a 1M concentration of FeCl3 for 10 hrs and HNO3 for 20 minutes, respectively. After the Ni-etching process, the transferred wafer was rinsed with DI water and blown with purified N2 gas. Finally, as seen in Fig. 2(c), a top Ni/Au electrode contact with an interdigitated pattern was fabricated on top of the transferred GaN active layer and underwent deep-ultraviolet sensing analysis. The fabricated device has dimension of 0.08 x 0.039 cm^2 and the active area of 0.6 x 10^{-3} cm^2. An optical microscope, UV-Vis measurement systems (Hewlett Packard 8453), and photoluminescence measurement utilizing a SpectraPro-300i monochromator (Acton) and He-Cd laser with an output of 10 mW power at room temperature were conducted to examine the surface morphology and optical properties of all transferred layers. The current-voltage (I-V) characteristics were assessed under illumination from a 254 nm UV light-emitting diode (LED) utilizing a semiconductor characterization system (Keithley 4200-MS Tech).

3. Results and Discussion

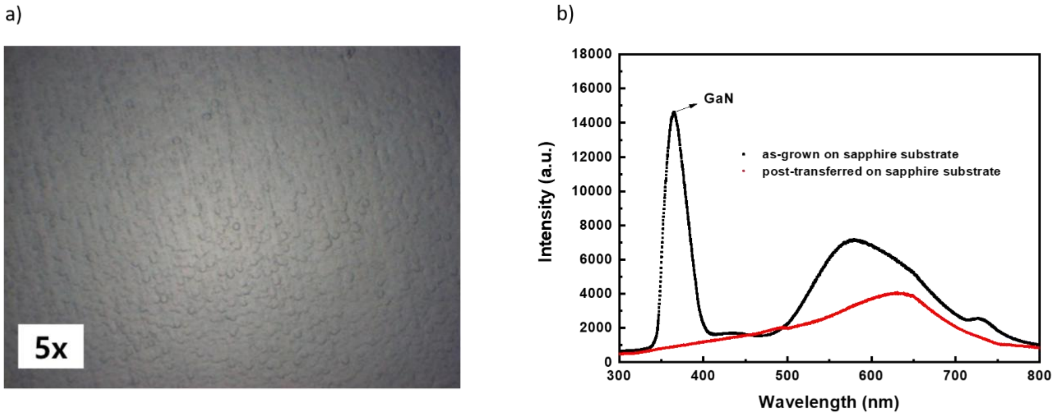

Figure 3. a) The optical microscope image of the GaN/h-BN surface on sapphire substrate and b) The PL spectra measured from sapphire substrate before and after GaN lift-off process.

The surface image of the GaN/h-BN/sapphire was viewed through an optical microscope (OM) at low magnification (5x) in Fig. 3(a). We can see that the epitaxial GaN layer, which is grown on a two-dimensional h-BN layer, has evenly spread hillock defects in a line across the whole surface. There are two primary factors that are likely to be responsible for hillock defects. Grain boundaries form near dislocations and the surface layer experiences stress. The hillock defects were caused by the way GaN started to form on the h-BN release layer, especially in areas with a lot of gallium. In fact, surrounding the Ga-rich regions, the trend of growth aims to balance the stress on the surface, which originated from Ostwald ripening. However, the GaN hillock grows without reaching the critical radius of Ostwald ripening, as demonstrated by Li, Tianbao et al., about the growth mechanism of GaN epitaxial layers on graphite [29]. The uniform stripes on GaN surface grown on two-dimensional material are due to a lack of well-defined crystallographic planes, presenting a type of surface defect, as has been demonstrated by D. Liang et al., which impacts morphology surface in this experiment result [24]. Numerous tripes as resemble step-terrace characteristics with a little inclination toward parallel alignment can still been seen, however, they were not noticeable or continuous. These weakly parallel patterns pointed to a restricted impact from the sapphire substrate. It implied that the direct transfer of the substrate lattice potential was greatly attenuated. Also, the absence of a mosaic structure indicated that the h-BN release layer improved the crystal quality of GaN by reducing the twist and tilt angles at the grain boundaries and helps solve issues that come up when growing a GaN layer on sapphire substrates [18, 31-33]. Seeing clear hillock defects all over the surface suggested that the h-BN layer effected to crystalline GaN growth. It is consistent with the previous report [25]. Photoluminescence spectroscopy was measured from the sapphire substrate before and after GaN was transferred to verify the presence and optical properties of GaN, as shown in Fig. 3(b). In the as-grown sample, a strong emission peak was observed at approximately 364 nm that refers to the optical bandgap energy of GaN (3.41 eV) as-grown on a sapphire substrate [28, 34]**.** The broad emission peak from 500 to 800 nm was attributed to the defect-related gaps generated during quasi-van der Waals epitaxial of 2D h-BN on 3D sapphire substrates. It is clear to see that the GaN characteristic emission peak vanished after GaN was removed from the sapphire substrate, as shown in the red solid line. This observation proved that GaN was successfully lifted off from the sapphire substrate. It also experimentally reveals the weak interfacial bonding between GaN and 2D h-BN.

The quarter-wafer scale, OM pictures, and UV-Vis of the first stage following the mechanical removal of the GaN using a 700-nm-thick Ni stressor layer on top are shown in Figs. 4 (a-c). Following the initial step of the transfer procedure, the surface morphology of the flexible handle tape and sapphire substrate are indicated by the blue and red square markers, respectively. A clean boundary image between h-BN/sapphire and the remaining Ni stressor layer was seen on the sapphire substrate in Fig. 4(a). Furthermore, as seen in Fig. 4(b), the UV-Vis was also performed to verify the elimination of GaN. It was carried out between 200 and 800 nm in the visible and ultraviolet spectrum, and the bandgap value was also determined using the Tauc plot equation. The absorption occurred in the 200–300 nm range, which corresponds to a bandgap of 5.65 eV. This bandgap value is typical of h-BN material [35, 36]. This finding verified that h-BN was the only material left on the wafer after the Ni/GaN layer was successfully removed from the sapphire substrate. The interfacial fracture that results in the selective separation of GaN and h-BN/sapphire is easily caused by the weak vdW bonding at the GaN/h-BN interface. The remote epitaxy mode-enabled transmission is consistent with this phenomenon [21]. Nonetheless, the large-area surface that was seen upon transfer and the ease of delamination suggest that a control mechanism akin to remote epitaxy is in place. We discovered that the Ni layer's aided function was responsible for this phenomenon.

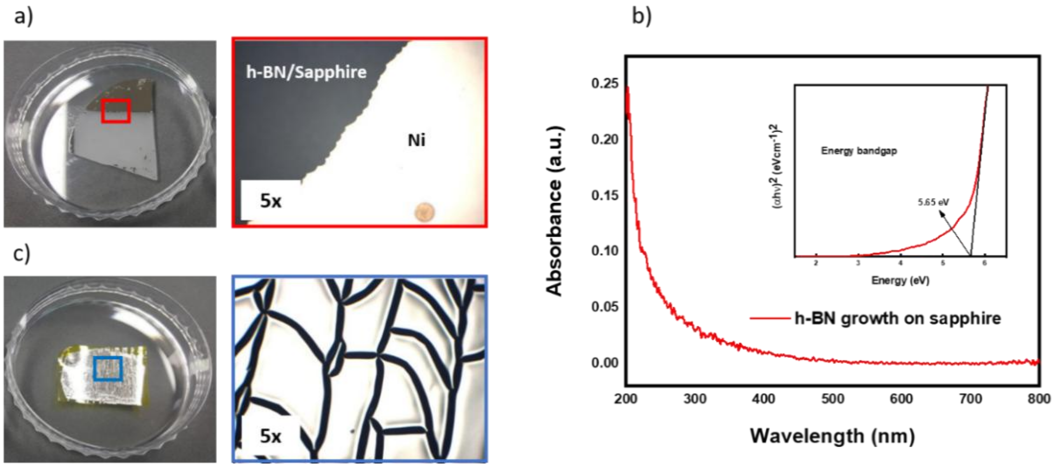

Figure 4. a) The surface image on sapphire substrate after transfer; b) The UV-Vis image after transfer on sapphire substrate and c) The surface image Ni/GaN on flexible handle tape.

Fig. 4(c) shows a surface picture of the Ni/GaN layer on flexible handle tape, measuring approximately 2.5 cm by 2.5 cm. The Ni/GaN layer was completely affixed to a flexible tape with several bowings on the surface Ni layer beneath the transparent surface, as seen in the experimental photograph. The OM measurement was applied to the Ni/GaN surface on flexible handle tape in order to examine the interaction between the GaN layer, Ni, and h-BN-assisted. The Ni layer's surface showed many cracks and surface bending, which were signs of stress-induced alterations in surface morphology. Based on the findings presented by SW, Bedell et al. [35], the mechanic has provided an explanation. The distribution of internal forces (intrinsic stress) between and within GaN, Ni, and h-BN under external pressures such as shocks, bending, and compressive loading at adhesive tape is the source of these alterations. This mechanism will cause a spontaneous fracture parallel to the layer interface. Additionally, we first determined that this technique will affect the GaN quality below using the surface Ni; the crucial goal is met. Therefore, balanced stress relaxation at the weak vdWs GaN/h-BN allowed for the successful GaN transfer. The method's dependability was further illustrated by the undamaged h-BN surface on sapphire following lift-off.

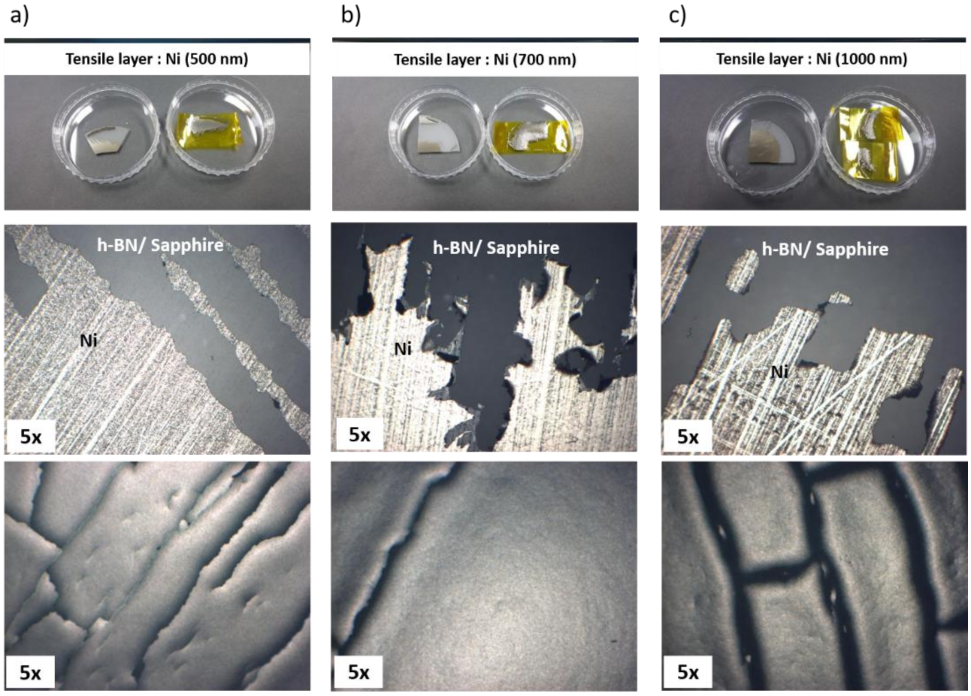

Figure 5. The top-view images depend on Ni layer thickness a) 500 nm; b) 700 nm; and c) 1000 nm.

When the GaN/h-BN layer breaking is beginning, it was thought that the thickness of the Ni layer, also referred to as the stressor layer, significantly affects transfer efficiency [19], [28]. Thus, as illustrated in Fig. 5, various Ni stressor layer thicknesses, including 500 nm, 700 nm, and 1000 nm, were carried out here while maintaining the same GaN/h-BN in order to elucidate and optimize the impact of Ni stressor layer thickness on the transferred GaN process. In this case, the Ni layer functions as an aided membrane that promotes fracture by lowering the uneven surface stress and creating interior stress. The Ni stressor layer, which is 700 nm thick, exhibits the most consistent and flawless GaN transfer across a wide region among the samples. Stated differently, the 700 nm-thick sample showed a lower crack density than the 500 nm and 1000 nm samples depicted in Figs. 5(a) and 5(c). There were many fissures on the GaN surface that were spreading in various directions. Specifically, GaN fractures were deep fissures and separations between regions with a thickness of 1000 nm. The imbalance of stress and compressive forces along the entire surface is indicative of improperly adjusted Ni layer thickness. Incomplete delamination results from irregular rolling, bending, and shearing at the cleaving plane during lift-off. As a result, the GaN membrane is severely cracked by the vdWs h-BN layer and GaN contact. A Ni stressor layer 700 nm thick was thought to be the ideal thickness because it had the lowest crack density; as a result, it was later used to fabricate the flexible UV sensor.

To ascertain the optical integrity of GaN, the PL spectroscopy is evaluated on the GaN/PET substrate, as shown in Fig. 6. The emission peak of GaN persisted on PET, indicating less strain distribution at the membrane, retained optical properties, and crystalline purity [36]. On the other hand, the GaN peak's intensity considerably dropped and its broadened little. In addition to surface-related flaws and the impact of mechanical strain, the behavior can be ascribed to the two-step transfer method that significantly decreased the GaN thickness [14, 36]. The broad emission peak, which corresponds to the PET substrate, was also observed in the 600–750 nm region. Regarding these findings, GaN was entirely extracted from sapphire and maintained its optical characteristics on PET substrates following a two-step mechanical lift-off.

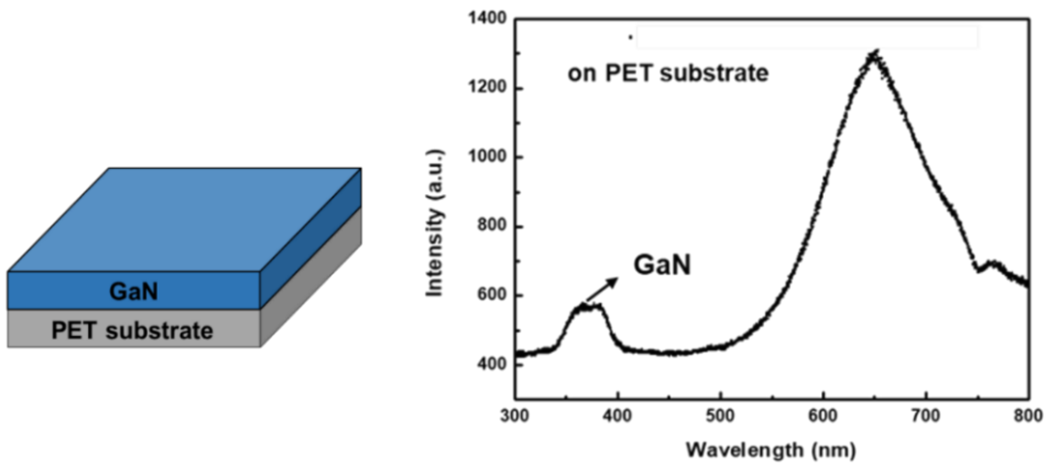

Figure 6. The PL spectra measured from the transferred GaN layer on PET substrate.

As seen in Fig. 7(a), a top interdigitated Ni/Au electrode on a GaN layer was deposited onto a PET substrate to create a flexible deep-ultraviolet sensor for practical use. The current–voltage (I–V) characteristics of fabricated GaN-on-PET device were measured in both dark and 254 nm light. The dark current density was 0.366 nA/cm² at -20 V, whereas its photocurrent density was 1.09 nA/cm² at the same voltage (Fig. 7(b)).

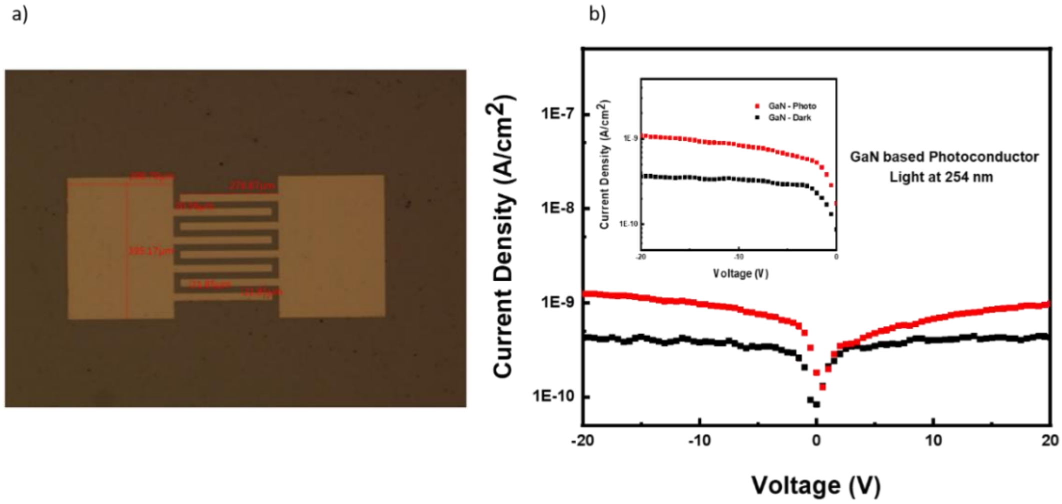

Figure 7. The I-V characteristics of the transferred GaN on PET substrate under DUV illumination.

The time response of the GaN-on-PET samples at a bias of -20V and -30V, under irradiation by the 254 nm LED light source, is depicted in Fig. 8(a). It is evident that the dynamic response of the prepared device is unsaturated as a result of the persistent photoconductivity phenomenon. Nevertheless, the time cycle (on/off) for light irradiation was preserved to differentiate the photocurrent changes when the applied voltage increased from -20V to -30V. The responsivity of the GaN-on-PET sensor at a bias of -20 V was measured as a function of the excitation wavelength, as illustrated in Fig. 8(b). The fabricated device is evidently sensitive to UV radiation within the 200 nm to 260 nm range, with the highest response occurring in the UVC region. This result is consistent with the excitation wavelength that was chosen for this investigation.

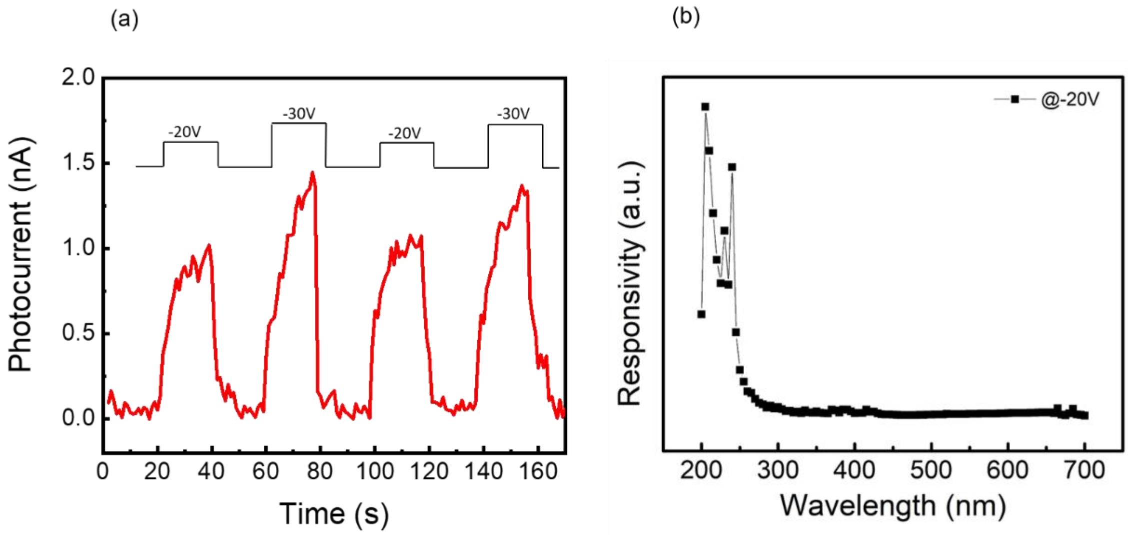

Figure 8. a) Time-response of the GaN-on-PET samples at a bias of -20V and -30V, and under 254 nm excitation wavelength; b) Responsivity curve of the GaN-on-PET sample measured as a function of exciation wavelength.

Table 1. Comparison of various GaN-based UV sensors on different substrates

Properties							
Material	Material integration approach	Light illumination (nm)	Responsivity (A W^{-1})	Detectivity (Jones)	Current ratio	Dark current (A)	Active area (cm^2)
GaN/PET (this work)	Mechanical transfer	254	-	-	2.97	3.66 $x10^{-10}$	0.6 x 10^{-3}
GaN/sapphire [37]	Direct growth	365	151.62	2.15x10^{13}	10^6	10.5 $x10^{-12}$	81
GaN/F-mica [38]	Direct growth	365	0.3	-	-	-	-
GaN/AlN/Si [39]	Direct growth	325	35.4	-	-	12 $x10^{-9}$	1.18 $x10^{-3}$
ZnO-a-Ga_2O_3/PET [40]	Microwire transfer	254	88.7x10^{-3}	-	-	-	8x10^{-5}
Ga_2O_3/flexible substrate [41]	Mechanical transfer	250	17x10^{-3}	-	-	-	16.2
ZnO/PET [42]	DSET transfer	365	-	-	431	-	-

The device likely had a low on/off ratio. However, a straightforward mechanical lift-off technique was used to transfer the GaN layer to a flexible substrate; in particular, the sensor was successfully studied in the deep UV region. GaN's photoresponse on PET performs similar to that of other UV sensors (Table 1). It suggested that simple mechanical lift-off of the GaN layer is made possible by the combination of the Ni stressor layer and the 2D h-BN release layer, enabling the practical implementation of flexible GaN-based DUV sensors.

4. Conclusion

In summary, the combination of the Ni stressor and h-BN release layer enables mechanical lift-off and transferred GaN on PET substrate. The optical microscope measurement revealed that the Ni stressor thickness strongly influences the cracked surface during the mechanical lift-off process, and the 700-nm-thick Ni was the best optimized thickness for minimal cracking on the GaN surface. Photoluminescence and UV-Vis measurements implied that the value of the optical bandgap of GaN was still retained after lift-off and being transferred to flexible PET substrate. The transferred GaN on PET substrate was utilized to fabricate a flexible DUV sensor with interdigitated top Ni/Au electrodes. Under excitation light of 254 nm, the photoresponse shows an on/off ratio of 2.97 with a low current density of 10^{-9}A. A stress-engineered mechanical lift-off incorporated with a 2D-h-BN release layer suggests a practical approach to realizing the remote epitaxy GaN-based optoelectrical devices, especially flexible UV sensors.

CRediT Authorship Contribution Statement

N. H. Hung and N. T. Trang: Investigating, Writing – original draft, Data curation, Formal analysis. K. B. Ko and H. V. A. Hao: Conceptualization, Visualization. T. V. Cuong: Visualization, Writing – review & editing. H. T. M. Hoa: Resources, Supervision, Writing – review & editing.

Acknowledgments

This research was funded by the Nguyen Tat Thanh University (NTTU) under grant number 2025.01.211/HĐ-KHCN. Research facilities and equipment were supported by Nguyen Tat Thanh University, Ho Chi Minh City, Vietnam.

References

[1] M. S. Kang, C. H. Lee, J. B. Park, H. Yoo, G. C. Yi, Gallium Nitride Nanostructures for Light-Emitting Diode Applications, Nano Energy, Vol. 1, No. 3, 2012, pp. 391-400, https://doi.org/10.1016/j.nanoen.2012.03.005.

[2] A. Udabe, I. Baraia, D. Garrido, Gallium Nitride Power Devices: A State of the Art Review, IEEE Access, Vol. PP, 2023, pp. 1-1, https://doi.org/10.1109/ACCESS.2023.3277200.

[3] M. D. Vecchia, S. Ravyts, G. V. D. Broeck, J. Driesen, Gallium-Nitride Semiconductor Technology And Its Practical Design Challenges in Power Electronics Applications: An Overview, Energies, Vol. 12, No. 14, 2019, pp. 2663, https://doi.org/10.3390/en12142663.

[4] F. Cao, Y. Liu, M. Liu, Z. Han, X. Xu, Q. Fan, B. Sun, Wide Bandgap Semiconductors for Ultraviolet Photodetectors: Approaches, Applications, and Prospects, Research, Vol. 7, 2024, pp. 0385, https://doi.org/10.34133/research.0385.

[5] N. Aggarwal, G. Gupta, Enlightening Gallium Nitride-Based UV Photodetectors, Journal of Materials Chemistry C, Vol. 8, No. 36, 2020, pp. 12348-12354, https://doi.org/10.1039/D0TC03219K.

[6] N. 'Adnin A. Zulkifli, K. Park, J. W. Min, B. S. Ooi, R. Zakaria, J. Kim, C.L. Tan, A Highly Sensitive, Large Area, And Self-Powered UV Photodetector Based on Coalesced Gallium Nitride Nanorods/Graphene/Silicon (111) Heterostructure, Applied Physics Letters, Vol. 117, No. 19, 2020, pp. 191103, https://doi.org/10.1063/5.0018076.

[7] O. A. Zuhairi, A. Shuhaimi, N. Nayan, A. Azman, A. Kamarudzaman, O. Alobaidi, M. Ghanim, E.T. Abdullah, Y. Zhu, Non-Polar Gallium Nitride for Photodetection Applications: A Systematic Review, Coatings, Vol. 12, No. 2, 2022, pp. 275, https://doi.org/10.3390/coatings12020275.

[8] W. W. Moses, Photodetectors for Nuclear Medical Imaging, Nuclear Instruments and Methods in Physics Research Section A: Accelerators, Spectrometers, Detectors and Associated Equipment, Vol. 610, No. 1, 2009, pp. 11-15, https://doi.org/10.1016/j.nima.2009.05.032.

[9] S. Liu, X. Wang, N. Xu, R. Li, H. Ou, S. Li, Y. Zhu, Y. Ke, R. Zhan, H. Chen, S. Deng, A Flexible And Wearable Photodetector Enabling Ultra-Broadband Imaging from Ultraviolet to Millimeter-Wave Regimes, Advanced Science, Vol. 11, No. 26 , 2024, pp. 2401631, https://doi.org/10.1002/advs.202401631.

[10] W. Fang, Q. Li, J. Li, Y. Li, Q. Zhang, R. Chen, M. Wang, F. Yun, T. Wang, Deep Ultraviolet Photodetector: Materials and Devices, Crystals, Vol. 13, No. 6, 2023, pp. 915, https://doi.org/10.3390/cryst13060915.

[11] E. O. Polat, G. Mercier, I. Nikitskiy, E. Puma, T. Galan, S. Gupta, M. Montagut, J.J. Piqueras, M. Bouwens, T. Durduran, G. Konstantatos, S. Goossens, F. Koppens, Flexible Graphene Photodetectors for Wearable Fitness Monitoring, Science Advances, Vol. 5, No. 9, 2019, pp. 7846, https://doi.org/10.1126/sciadv.aaw7846.

[12] R. H. Jiang, C. F. Lin, Y. C. Huang, F. H. Fan, K. C. Wu, J. H. Wang, P. F. Cheng, C. C. Yang, Separating InGaN Membranes from GaN/Sapphire Templates through A Crystallographic-Etch-Limited Process, RSC Advances, Vol. 3, No. 32, 2013, pp. 13446-13450, https://doi.org/10.1039/C3RA41811A.

[13] ResearchGate, Wet-Chemical Etching of GaN: Underlying Mechanism of A Key Step in Blue And White LED Production | Request PDF, https://www.researchgate.net/, 2025 (accessed on: February 11th , 2025).

[14] P. Gu, S. Yang, L. Ma, T. Yang, X. Hou, Y. Mei, L. Ying, H. Long, B. Zhang, Flexible GaN-Based Ultraviolet Microdisk Lasers on PET Substrate, Optics Letters, Vol. 48, No. 15, 2023, pp. 4117-4120, https://doi.org/10.1364/OL.496680.

[15] T. Ueda, M. Ishida, M. Yuri, Separation of Thin GaN from Sapphire by Laser Lift-Off Technique, Japanese Journal of Applied Physics, Vol. 50, No. 4R, 2011, pp. 041001, https://doi.org/10.1143/JJAP.50.041001.

[16] K. Jang, J. Heo, Fast and Highly Selective GaN-over-AlGaN Etching with Low Surface Damage, Journal of Semiconductor Technology and Science, Vol. 26, No. 1, 2026, pp. 16-23.

[17] W. H. Jang, K. S. Seo, H. Y. Cha, P-GaN Gated AlGaN/GaN E-Mode HFET Fabricated with Selective GaN Etching Process, 2020, https://doi.org/10.5573/JSTS.2020.20.6.485.

[18] Y. Kobayashi, K. Kumakura, T. Akasaka, T. Makimoto, Layered Boron Nitride as A Release Layer for Mechanical Transfer of GaN-based Devices, Nature, Vol. 484, Nol. 7393, 2012, pp. 223-227, https://doi.org/10.1038/nature10970.
[19] C. H. Cheng, T. W. Huang, C. L. Wu, M. K. Chen, C. H. Chu, Y. R. Wu, M. H. Shih, C. K. Lee, H. C. Kuo, D. P. Tsai, G. R. Lin, Transferring The Bendable Substrateless GaN LED Grown on A Thin C-Rich SiC Buffer Layer to Flexible Dielectric and Metallic Plates, Journal of Materials Chemistry C, Vol. 5, No. 3, 2017, pp. 607-617, https://doi.org/10.1039/C6TC04318F.
[20] L. Wang, S. Yang, F. Zhou, Y. Gao, Y. Duo, R. Chen, J. Yang, J. Yan, J. Wang, J. Li, Y. Zhang, T. Wei, Wafer-Scale Transferrable GaN Enabled by Hexagonal Boron Nitride for Flexible Light-Emitting Diode, Small, Vol. 20, No. 7, 2024, pp. 2306132, https://doi.org/10.1002/smll.202306132.
[21] F. Dross, J. Robbelein, B. Vandevelde, E. Van Kerschaver, I. Gordon, G. Beaucarne, J. Poortmans, Stress-Induced Large-Area Lift-Off of Crystalline Si Films, Applied Physics A, Vol. 89, No. 1, 2007, pp. 149-152, https://doi.org/10.1007/s00339-007-4195-2.
[22] Y. Kim, S. S. Cruz, K. Lee, B. O. Alawode, C. Choi, Y. Song, J. M. Johnson, C. Heidelberger, W. Kong, S. Choi, K. Qiao, I. Almansouri, E. A. Fitzgerald, J. Kong, A. M. Kolpak, J. Hwang, J. Kim, Remote Epitaxy through Graphene Enables Two-Dimensional Material-Based Layer Transfer, Nature, Vol. 544, No. 7650, 2017, pp. 340-343, https://doi.org/10.1038/nature22053.
[23] B. I. Park, J. Kim, K. Lu, X. Zhang, S. Lee, J.M. Suh, D. H. Kim, H. Kim, J. Kim, Remote Epitaxy: Fundamentals, Challenges, and Opportunities, Nano Letters, Vol. 24, No. 10, 2024, pp. 2939-2952, https://doi.org/10.1021/acs.nanolett.3c04465.
[24] D. Liang, T. Wei, J. Wang, J. Li, Quasi Van Der Waals Epitaxy Nitride Materials and Devices on Two Dimension Materials, Nano Energy, Vol. 69, 2020, pp. 104463, https://doi.org/10.1016/j.nanoen.2020.104463.
[25] M. Han, B. D. Ryu, K.B. Ko, C. H. Hong, Quasi-Van Der Waals Epitaxial Growth of GaN on Hexagonal Boron Nitride via Metal-Organic Chemical Vapor Deposition, Physica Status Solidi B Basic Research, Vol. 260, No. 8. 2023, pp. 2200496, https://doi.org/10.1002/pssb.202200496.
[26] A. Koma, Van Der Waals Epitaxy- A New Epitaxial Growth Method for A Highly Lattice-Mismatched System, Thin Solid Films, Vol. 216, No. 1, 1992, pp. 72-76, https://doi.org/10.1016/0040-6090(92)90872-9.
[27] M. Tokarczyk, A. K. Dąbrowska, G. Kowalski, R. Bożek, J. Iwański, J. Binder, R. Stępniewski, A. Wysmołek, Effective Substrate for The Growth of Multilayer h-BN on Sapphire-Substrate Off-Cut, Pre-Growth, and Post-Growth Conditions in Metal-Organic Vapor Phase Epitaxy, 2D Mater, Vol. 10, No. 2, 2023, pp. 025010, https://doi.org/10.1088/2053-1583/acb44a.
[28] A. H. Park, T. H. Seo, Hexagonal Boron Nitride as An Intermediate Layer for Gallium Nitride Epitaxial Growth in Near-Ultraviolet Light-Emitting Diodes, Materials, Vol. 16, No. 22, 2023, pp. 7216, https://doi.org/10.3390/ma16227216.
[29] T. Li, C. Liu, Z. Zhang, B. Yu, H. Dong, W. Jia, Z. Jia, C. Yu, L. Gan, B. Xu, H. Jiang, Understanding the Growth Mechanism of GaN Epitaxial Layers on Mechanically Exfoliated Graphite, Nanoscale Research Letters, Vol. 13, No. 1, 2018, pp. 130, https://doi.org/10.1186/s11671-018-2546-x.
[30] US20220216109A1 - Stress-Induced Selective-Area Lift-Off of Thin Films And Devices on Van Der Waals Buffer Layers - Google Patents, (n.d.), https://patents.google.com/patent/US20220216109A1/en (accessed on: February 11th , 2025).
[31] F. Liu, Y. Yu, Y. Zhang, X. Rong, T. Wang, X. Zheng, B. Sheng, L. Yang, J. Wei, X. Wang, X. Li, X. Yang, F. Xu, Z. Qin, Z. Zhang, B. Shen, X. Wang, Hexagonal BN-Assisted Epitaxy of Strain Released GaN Films for True Green Light-Emitting Diodes, Advanced Science, Vol. 7, No. 21, 2020, pp. 2000917, https://doi.org/10.1002/advs.202000917.
[32] T. Ayari, S. Sundaram, C. Bishop, A. Mballo, P. Vuong, Y. Halfaya, S. Karrakchou, S. Gautier, P. L. Voss, J. P. Salvestrini, A. Ougazzaden, Novel Scalable Transfer Approach for Discrete III-Nitride Devices Using Wafer-Scale Patterned h-BN/Sapphire Substrate for Pick-and-Place Applications, Advanced Materials Technologies, Vol. 4, No. 10, 2019, pp. 1900164, https://doi.org/10.1002/admt.201900164.
[33] M. Hiroki, K. Kumakura, H. Yamamoto, Substrate-Transfer Technique Using h-BN for GaN-Based High-Power Transistors, NTT Technical Review, Vol. 14, No. 8, 2016, pp. 44-49, https://doi.org/10.53829/ntr201608ra1.
[34] B. J. Zhang, T. Egawa, G. Y. Zhao, H. Ishikawa, M. Umeno, T. Jimbo, Schottky Diodes of Ni/Au on n-GaN Grown on Sapphire And SiC Substrates, Applied Physics Letters, Vol. 79, No. 16, 2001, pp. 2567-2569, https://doi.org/10.1063/1.1410355.
[35] G. Cassabois, P. Valvin, B. Gil, Hexagonal Boron Nitride is an Indirect Bandgap Semiconductor, Nature Photon, Vol. 10, No. 4, 2016, pp. 262-266, https://doi.org/10.1038/nphoton.2015.277.

[36] J. Cao, T. L. Meng, X. Zhang, C. K. I. Tan, A. Suwardi, H. Liu, On Functional Boron Nitride: Electronic Structures And Thermal Properties, Materials Today Electronics, Vol. 2, 2022, pp. 100005, https://doi.org/10.1016/j.mtelec.2022.100005.

[37] H. Liu, Y. Wang, C. Liu, W. Gao, L. Han, X. Wang, J. Li, GaN-on-Sapphire Vertical Trench MOSFET Array with High-Performance Ultraviolet (UV) Photoresponse, ACS Applied Optical Materials, Vol. 1, No. 8, 2023, pp. 1485–1491. https://doi.org/10.1021/acsaom.3c00200.

[38] Y. Geng, Y. Xu, R. Li, X. Li, X. Wang, Q. Lin, H. Wu, C. Liu, Van Der Waals Epitaxy GaN on Fluorophlogopite Mica for Transfer-Free Flexible UV Photodetector, Materials Letters, Vol. 385, 2025, pp.138185,https://doi.org/10.1016/j.matlet.2025.138185

[39] L. Goswami, N. Aggarwal, P. Vashishtha, S. K. Jain, S. Nirantar, J. Ahmed, M. A. M. Khan, R. Pandey, G. Gupta, Fabrication of GaN Nano-Towers Based Self-Powered UV Photodetector, Scientific Reports, Vol. 11, No.1, 2021, pp. 10859, https://doi.org/10.1038/s41598-021-90450-w.

[40] Y. Liu, K. Liu, J. Yang, Z. Cheng, X. Chen, Y. Zhu, B. Li, L. Liu, D. Shen, A Self-Powered Flexible UV Photodetector Based on An Individual ZnO-Amorphous Ga_2O_3 Core–Shell Heterojunction Microwire, Journal of Materials Chemistry C, Vol. 12, No. 26, 2024, pp. 9623-9629, https://doi.org/10.1039/D4TC01327A.

[41] Y. Lu, S. Krishna, C. H. Liao, Z. Yang, M. Kumar, Z. Liu, X. Tang, N. Xiao, M. B. Hassine, S.T. Thoroddsen, X. Li, Transferable Ga_2O_3 Membrane for Vertical And Flexible Electronics via One-Step Exfoliation, ACS Applied Materials & Interfaces, Vol. 14, No. 42, 2022, pp. 47922-47930, https://doi.org/10.1021/acsami.2c14661.

[42] H. Jang, D. K. Kwon, D. H. Kim, J. M. Myoung, Characteristics of Flexible ZnO Nanorod UV Photodetectors Processed by Using A Direct Silicon Etching Transfer Method, Journal of Materials Chemistry C, Vol. 10, No. 17, 2022, pp. 6805-6811, https://doi.org/10.1039/D2TC00377E.